

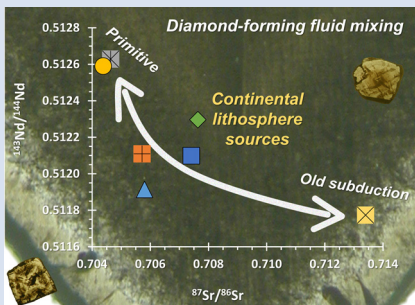
## Sr-Nd-Pb isotopes of fluids in diamond record two-stage modification of the continental lithosphere

Y. Weiss<sup>1\*</sup>, J.M. Koornneef<sup>2</sup>, G.R. Davies<sup>2</sup>



<https://doi.org/10.7185/geochemlet.2329>

### Abstract



High-density fluid (HDF) microinclusions in diamonds allow direct investigation of deep carbon- and water-rich fluids that influence the properties of Earth's mantle. Identifying the sources and evolution of such fluids in the context of different potential mantle reservoirs is difficult due to the limited radiogenic isotope data. Here, we report Sr-Nd-Pb isotope compositions of silicic to low-Mg carbonatitic HDFs in a suite of diamonds from a single source in Canada. Relationships between isotopes and trace element compositions indicate the contribution of two distinct sources within the continental lithosphere: one with relatively primitive isotopic compositions characterised by  $\epsilon\text{Nd}$  of  $-0.2$ ,  $^{87}\text{Sr}/^{86}\text{Sr}$  of  $0.7044$  and  $^{206}\text{Pb}/^{204}\text{Pb}$  of  $17.52$ , and another with more unradiogenic  $\epsilon\text{Nd} < -16$  and radiogenic  $^{87}\text{Sr}/^{86}\text{Sr}$  and  $^{206}\text{Pb}/^{204}\text{Pb} > 0.713$  and  $18.3$ , respectively. We suggest that the latter reflects an old metasomatic event in the continental lithosphere involving fluid addition from a subducting slab, most probably in the Paleoproterozoic. HDFs formed and their host diamonds crystallised in a more recent metasomatic event, indicated by the unaggregated nitrogen of the diamonds, where fluids from both sources mixed. HDFs from Canada, Botswana, and Congo have comparable isotope-trace element relationships, suggesting contributions of similar sources in distinct lithospheric provinces worldwide.

Received 25 April 2022 | Accepted 30 August 2023 | Published 20 September 2023

### Introduction

Carbon- and water-rich fluids involved in large-scale tectonic processes carry incompatible element-enriched chemical fingerprints, which are common in metasomatised mantle-derived samples (e.g., Dawson, 1984; Turner *et al.*, 2021). Diamonds are a primary target for studying mantle metasomatic processes, as they form during fluid-rock interaction and often encapsulate ambient minerals and high-density fluids (HDFs; either melt or supercritical fluid). The most common HDFs are found as microinclusions in 'fibrous diamonds' (a fast-growing form of diamond that is usually translucent or opaque with cuboid faces; see Graphical Abstract), which vary in composition between four major types: hydrous-silicic, rich in Si, Al, K and  $\text{H}_2\text{O}$ ; low-Mg carbonatitic and high-Mg carbonatitic, both rich in Ca, Mg, Fe, K and  $\text{CO}_2$ ; and hydrous-saline, rich in Cl, K, Na and  $\text{H}_2\text{O}$  (Weiss *et al.*, 2022a). These HDFs provide the opportunity to directly examine the nature of carbon- and water-rich media in the deep Earth and constrain their varying origins (e.g., Smith *et al.*, 2012; Klein-BenDavid *et al.*, 2014; Kempe *et al.*, 2021).

Radiogenic isotopes preserve their signature during mantle processes such as melting and immiscible separation, and are therefore an important tool in tracing mantle sources. Available HDFs Sr isotope data range between  $0.703$  to  $0.723$ , indicating sources ranging from 'depleted' oceanic mantle to old continental lithosphere (Akagi and Masuda, 1988; Klein-BenDavid *et al.*, 2010,

2014; Smith *et al.*, 2012; Weiss *et al.*, 2015). To date, only a handful of diamond HDFs have been analysed for their Nd and Pb isotope compositions ( $n = 5$  and  $3$ , respectively; Klein-BenDavid *et al.*, 2010, 2014), which hinders unambiguous evaluation of possible mantle sources or recycled surface materials in metasomatic events.

Here, we combine major, trace element and Sr-Nd-Pb isotope compositions of a suite of 7 HDF-bearing fibrous diamonds from Canada to constrain their petrogenesis. Together with the available isotopic data of similar HDF types in diamonds from different lithospheric provinces, we investigate possible HDF origin in the context of large-scale mantle reservoirs and processes, which control the spectrum of HDF compositions and the long-term evolution of the deep carbon cycle.

### Samples and Methods

Seven fibrous diamonds from a single source in Canada (exact origin is unknown; see Supplementary Information, Sample Description) were cut by laser to create  $\sim 500$   $\mu\text{m}$  slabs, polished on both sides, and analysed for their nitrogen characteristics and microinclusion compositions. FTIR (Fourier-transform infrared) spectroscopy establishes they carry 850 to 1250 ppm nitrogen and all exclusively exhibit absorption due to nitrogen in A-centers (a neighbouring pair of substitutional N atoms; pure Type IaA

1. The Freddy and Nadine Herrmann Institute of Earth Sciences, The Hebrew University of Jerusalem, Jerusalem 91904, Israel

2. Vrije Universiteit Amsterdam, Faculty of Science, De Boelelaan 1085, 1081 HV Amsterdam, The Netherlands

\* Corresponding author (email: yakov.weiss@mail.huji.ac.il)



spectrum). Major element compositions were determined by EPMA (Electron probe micro-analysis, [Kempe et al., 2021](#); [Weiss et al., 2022a](#)). We used the ‘diamond-in-water’ ablation approach to prepare the samples for solution trace element analyses by ICP-MS (Inductively coupled plasma mass spectrometry) and isotope analyses by TIMS (Thermal ionisation mass spectrometry, [Weiss et al., 2022b](#)). As total procedural blanks (TPBs) were too small for the determination of isotope compositions, all isotopic data are presented as measured values. Additional details are given in the [Supplementary Information](#).

### High-Density Fluid (HDF) Compositions

Major element compositions of microinclusions in the studied diamonds vary from silicic to low-Mg carbonatitic HDFs and fall within the range of HDF types in fibrous diamonds globally ([Fig. 1a](#)). They display a characteristic negative correlation between SiO<sub>2</sub> and CaO, as well as negative covariance between SiO<sub>2</sub> and FeO. There are positive relationships between SiO<sub>2</sub> and Al<sub>2</sub>O<sub>3</sub> as well as CaO and P<sub>2</sub>O<sub>5</sub>. K<sub>2</sub>O is relatively uniform ([Table S-1](#)), but correlates positively with Cl and negatively with MgO. No systematic spatial (core to rim) compositional change is observed and in most cases microinclusions within a single diamond show variation ≤15 % (1σ) for SiO<sub>2</sub> and K<sub>2</sub>O, and ≤20 % for CaO ([Table S-1](#)).

The trace element compositions of the HDFs ([Table S-2](#)) were published previously by [Weiss et al. \(2022b\)](#). Their primitive mantle (PM) normalised patterns are mostly similar and comparable to previously analysed HDFs ([Fig. 1b](#)). They exhibit overall decreasing levels from the most incompatible to compatible elements with characteristic anomalies (negative in most cases) of Rb, Nb, Sr, Zr, Hf and Ti, and trace element ratios indicating the involvement of accessory mantle phases in their formations ([Weiss et al., 2013](#)). There are no distinctive differences in trace element compositions between the silicic to low-Mg carbonatitic compositions; some trace element ratios show continuous variations irrespective of the major element compositional change (e.g., La/Nb, Zr/Eu; [Fig. 1, 2c](#); [Table S-2](#)).

The HDF's Sr and Nd isotope compositions vary between <sup>87</sup>Sr/<sup>86</sup>Sr = 0.70438 ± 1 (2SE) to 0.71340 ± 3 and <sup>143</sup>Nd/<sup>144</sup>Nd = 0.5126 ± 1 to 0.51177 ± 3 (εNd = -0.2 to -16.9; [Fig. 2a](#);

[Table S-3](#)). They show a general inverse Sr-Nd isotope correlation from bulk silicate Earth (BSE; [Zindler and Hart, 1986](#)) and South African kimberlite ([Becker and Le Roex, 2006](#)) values to more radiogenic <sup>87</sup>Sr/<sup>86</sup>Sr and unradiogenic <sup>143</sup>Nd/<sup>144</sup>Nd ratios, which trend through South African olivine lamproites (formerly Group II kimberlites or orangeite; [Becker and Le Roex, 2006](#)) towards the range of continental crust compositions ([Rudnick, 1990](#); [Thompson et al., 2007](#)). <sup>147</sup>Sm/<sup>144</sup>Nd ratios vary between 0.0669 ± 2 to 0.0970 ± 1 and show a general negative relationship with <sup>143</sup>Nd/<sup>144</sup>Nd ([Fig. 2b](#); [Table S-3](#)). The analysed diamond samples with a TPB contribution of <10 % for Pb (4 of 7; [Table S-3](#)), vary between 17.516 ± 2 and 18.149 ± 3 for <sup>206</sup>Pb/<sup>204</sup>Pb, 15.53 ± 3 and 15.680 ± 3 for <sup>207</sup>Pb/<sup>204</sup>Pb and 37.424 ± 6 and 38.412 ± 8 for <sup>208</sup>Pb/<sup>204</sup>Pb. These Pb isotope variations are between depleted to enriched mantle components for <sup>208</sup>Pb/<sup>204</sup>Pb vs. <sup>206</sup>Pb/<sup>204</sup>Pb, but extend to more radiogenic <sup>207</sup>Pb/<sup>204</sup>Pb values above the Pb mantle array ([Fig. S-1](#); [Hart et al., 1992](#); [Stracke, 2012](#)). They exhibit a strong positive correlation with Sr isotope compositions ([Fig. 3](#)).

The samples define a broad linear negative correlation between <sup>143</sup>Nd/<sup>144</sup>Nd and La/Nb ([Fig. 2c](#)). Similar inverse relationships are observed between <sup>143</sup>Nd/<sup>144</sup>Nd and La/Rb or La/Zr, whereas direct relationships are observed with Sr\* (Sr/√(Pr×Nd)) and Zr/Eu ratios (not shown; [Tables S-2, S-3](#)). Sr and Pb isotopes plotted against the same trace element ratios exhibit opposite correlations to those with Nd isotopes. These relationships are consistent with the general positive relationship between Sr isotopes and (La, Ba)/(Nb, Zr) ratios in HDFs ([Klein-BenDavid et al., 2014](#)). In comparison, no relationship is observed between Sr, Nd, or Pb isotopes and major element compositions; for example, HDF of silicic and low-Mg carbonatitic compositions (diamond 505 and 508) have almost identical Sr and Nd isotope ratios, whereas similar silicic HDFs (diamond 502 and 505) exhibit varying isotopic compositions ([Fig. 1, 2, 3](#); [Tables S-1, S-3](#)). These major element-radiogenic isotope systematics are similar to the decoupling between major and trace elements of HDFs from different lithospheric provinces worldwide ([Weiss et al., 2022a](#)).

Considering the concentration and unaggregated nature of nitrogen in the studied diamonds, and a likely average mantle residence temperature of ≥950 °C ([Stachel and Harris, 2008](#);

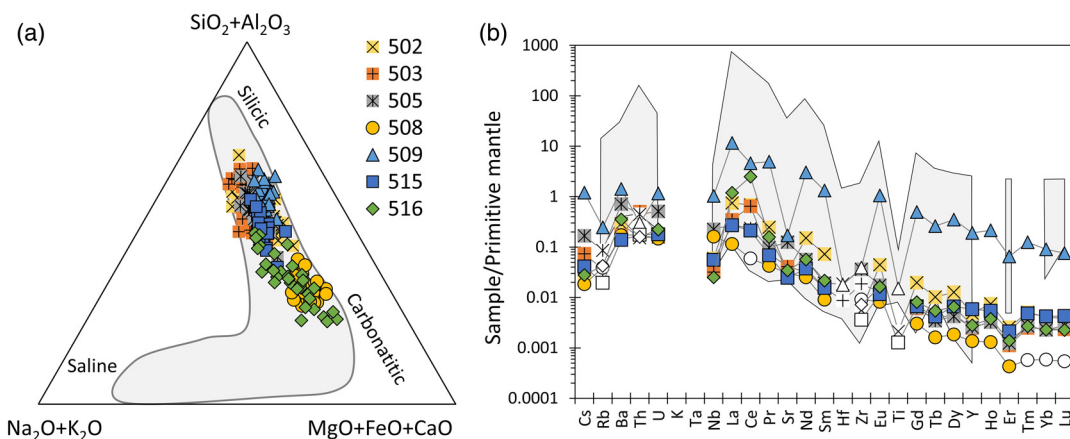


**Figure 1** Major and trace element composition of HDF microinclusions in fibrous diamonds. **(a)** SiO<sub>2</sub> + Al<sub>2</sub>O<sub>3</sub>–Na<sub>2</sub>O + K<sub>2</sub>O–MgO + FeO + CaO ternary diagram (in wt. %, on carbon- and water-free basis), showing the compositional range of HDFs in the studied diamonds (see key for sample symbols). Each datapoint represents an individual microinclusion. Data compared to the global variation between silicic, carbonatitic and saline HDF types (shaded area – [Weiss and Goldstein, 2018](#)). **(b)** Primitive mantle normalised ([McDonough and Sun, 1995](#)) trace element patterns of the HDFs compared to microinclusion-bearing diamonds (shaded area – [Klein-BenDavid et al., 2010, 2014](#)). White-filled symbols are data falling between LOQ and LOD (between 10× σ and 3× σ of the TPBs), and are regarded as qualitative (see details in the [Supplementary Information](#)).



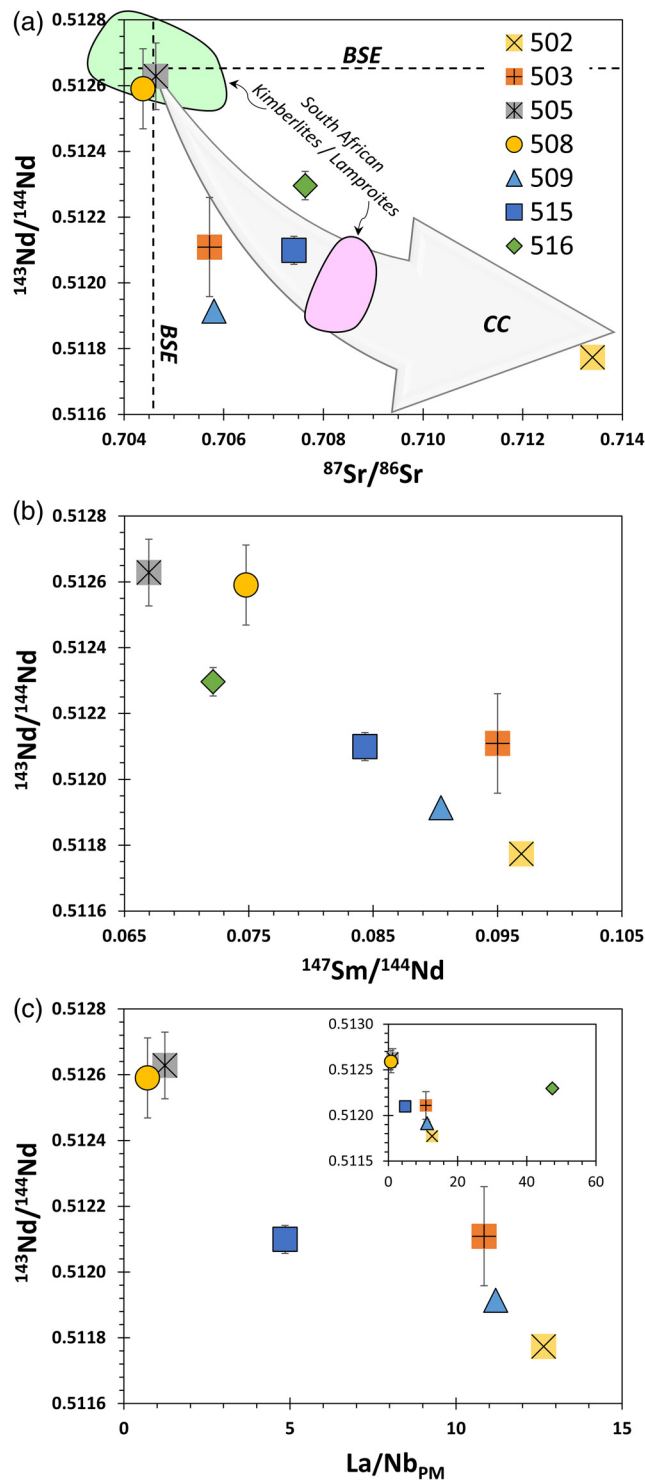


**Figure 2** Isotopic and trace element relationships of the HDFs. (a)  $^{143}\text{Nd}/^{144}\text{Nd}$  vs.  $^{87}\text{Sr}/^{86}\text{Sr}$ . Also plotted are the range of South African kimberlite and lamproites (Becker and Le Roex, 2006), bulk silicate Earth (BSE; Zindler and Hart, 1986), and the vector toward continental crust (CC arrow; Rudnick, 1990; Thompson et al., 2007). (b)  $^{143}\text{Nd}/^{144}\text{Nd}$  vs.  $^{147}\text{Sm}/^{144}\text{Nd}$ ; the latter is calculated from isotope dilution data (Table S-3). (c)  $^{143}\text{Nd}/^{144}\text{Nd}$  vs. primitive mantle normalised  $\text{La}/\text{Nb}_{\text{PM}}$  ratios; the inset includes diamond 516, which deviates from the general trend. Error bars represent  $\pm 2$  SE and in most cases are smaller than the symbols.

Weiss et al., 2022a), their formation could take place from immediately prior to kimberlite eruption up to a maximum of 1 Ga before eruption (Taylor et al., 1996). As the exact timing

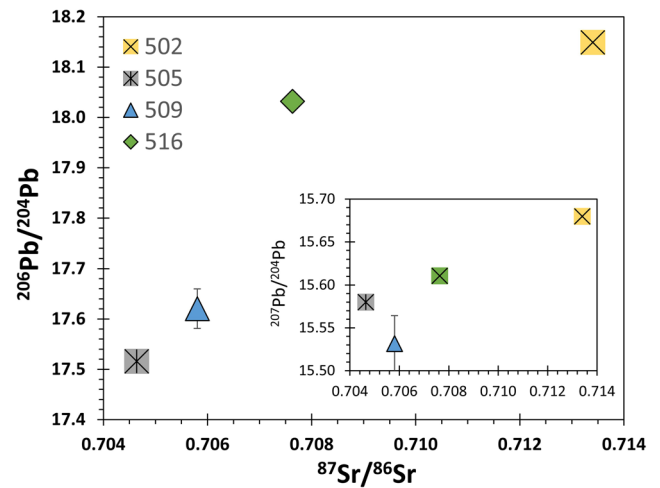


**Figure 3** Relationship between Pb and Sr isotope compositions of the HDFs.  $^{206}\text{Pb}/^{204}\text{Pb}$  ratios are shown in the main panel and  $^{207}\text{Pb}/^{204}\text{Pb}$  ratios in the inset. Error bars represent  $\pm 2$  SE, which in most cases are smaller than the symbols.

is unknown, a conservative correction for the isotopic composition of the HDFs is the possible range for the diamond emplacement age between 45–550 Ma, i.e. the age range of their possible Canadian host kimberlites (see Supplementary Information). Initial ratios corrected for 45 Ma are almost indistinguishable from measured values. Initial ratios based on 550 Ma are lower by 0.0005 to 0.0010 for  $^{87}\text{Sr}/^{86}\text{Sr}$  compared to the measured values, 0.00024 to 0.00035 for  $^{143}\text{Nd}/^{144}\text{Nd}$ , 0.009 to 0.116 for  $^{206}\text{Pb}/^{204}\text{Pb}$ , 0.0005 to 0.0068 for  $^{207}\text{Pb}/^{204}\text{Pb}$ , and 0.008 to 0.073 for  $^{208}\text{Pb}/^{204}\text{Pb}$  (Fig. 4). The important observation, however, is that the relationships and variations between Sr, Nd and Pb isotopes and between isotopes and trace element compositions persist and all samples have relatively high  $^{207}\text{Pb}/^{204}\text{Pb}$  (Figs. S1 and S2). This remains even if 1 Ga initial ratios are calculated.

### HDF Sources

The combined Sr-Nd-Pb isotope signature is not related to radiogenic ingrowth after HDFs were encapsulated in the diamonds during formation, but rather indicates the involvement of two sources with distinct isotopic compositions. This conclusion is established by the inverse correlation on the Sm-Nd isochron diagram (Fig. 2b), the spectrum of Sr and Nd isotopes and the linear relationship between Pb and Sr isotopes that indicate mixing of different endmember components (Fig. 2a and Fig. 3). The covariations of isotopic composition and trace element ratios further support mixing of two components (e.g., Fig. 2c). Klein-BenDavid et al. (2010, 2014) also argued for two-component mixing to explain the Sr isotope variations of HDFs, and suggested the involvement of convecting mantle and ancient sub-continental lithospheric mantle (SCLM). Indeed, an SCLM that experienced long-term LREE enrichment (low Sm/Nd) and increased Rb/Sr and U/Pb is required to explain the unradiogenic Nd and radiogenic Sr and Pb isotope endmember compositions of the HDFs studied here. However, the radiogenic  $^{207}\text{Pb}/^{204}\text{Pb}$  values of all of these HDFs, including those with Sr-Nd isotope compositions closest to BSE values, are significantly higher than the compositions of recent ocean island basalts. This is evidence of elevated U/Pb ratios in early Earth history for the source of both endmembers, and precludes major involvement of mantle of asthenospheric origin (Fig. S-1).





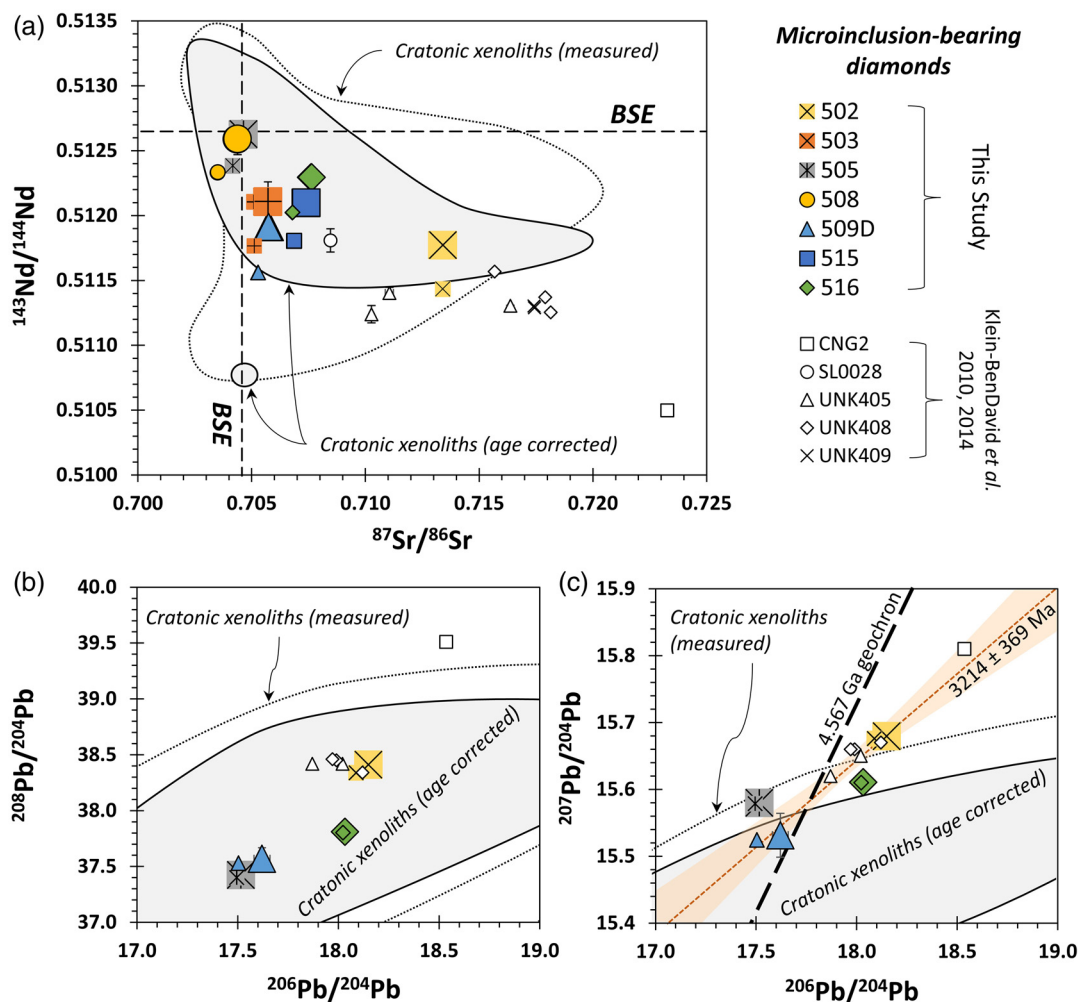


**Figure 4** Sr-Nd-Pb isotope compositions of HDF in fibrous diamonds. **(a)**  $^{143}\text{Nd}/^{144}\text{Nd}$  vs.  $^{87}\text{Sr}/^{86}\text{Sr}$ . Measured values (large coloured symbols) and initial ratios corrected for a maximum possible emplacement age of 550 Ma (small coloured symbols) are presented. Available published data for 5 diamonds from Botswana (UNK; all duplicate analyses are presented), Snap Lake (SL) and Congo (CNG) are also shown (small open symbols; Klein-BenDavid *et al.*, 2010, 2014). The isotopic range of cratonic continental lithosphere determined on whole rock xenolith data (dotted white area - measured values, and lined shaded area – age corrected initial values, based on the PetDB database; <http://www.earthchem.org/petdb>), and BSE (Zindler and Hart, 1986) are presented for comparison. **(b)**  $^{208}\text{Pb}/^{204}\text{Pb}$  vs.  $^{206}\text{Pb}/^{204}\text{Pb}$ , and **(c)**  $^{207}\text{Pb}/^{204}\text{Pb}$  vs.  $^{206}\text{Pb}/^{204}\text{Pb}$ ; symbols and areas as in **(a)**. The locus of compositions that developed undisturbed from primitive-mantle lead since Earth's formation is shown for reference (geochron; long dashed black line); the regression line through all the HDF data yields an age of  $3214 \pm 369$  Ma (dashed orange line and 95 % confidence interval).

Figure 4a shows that the Sr and Nd isotope spectrum of the SCLM, as inferred by global whole rock xenolith data from cratons, covers the complete isotopic range of the HDFs studied here. A comparable picture is revealed for  $^{208}\text{Pb}/^{204}\text{Pb}$  and  $^{206}\text{Pb}/^{204}\text{Pb}$  variations, but not for  $^{207}\text{Pb}/^{204}\text{Pb}$ , which reach higher values than recorded in SCLM whole-rock initial values (Fig. 4a,b). There is, however, evidence of ancient U enrichment in SCLM-derived xenoliths (Cohen *et al.*, 1984; Davies and Lloyd, 1986) and magmas (*i.e.* Western Australian lamproites; Fraser *et al.*, 1985) that are characterised by highly radiogenic  $^{207}\text{Pb}/^{204}\text{Pb}$  at relatively unradiogenic  $^{206}\text{Pb}/^{204}\text{Pb}$  compositions, some of which overlap the HDFs values.

A strong connection has previously been established between hydrous/carbonated eclogite lithologies (and pyroxenites) with silicic to low-Mg carbonatitic HDF types, comparable in composition to HDFs in the present study (Weiss *et al.*, 2022a). The Sr-Nd-Pb isotope compositions of eclogite and pyroxenite xenoliths (occasionally diamondiferous) are extremely diverse, from highly unradiogenic to highly radiogenic values (*e.g.*, Jacob, 2004; Xu *et al.*, 2009; Aulbach *et al.*, 2019). Although there

is limited available data from such xenoliths, their isotope variation overlaps most of the SCLM spectrum and HDFs (Fig. S-2). In addition, a large isotopic range was documented for eclogites from individual locations (Jacob, 2004; Aulbach *et al.*, 2019). Such sources for the HDF studied here can explain their silicic to low-Mg carbonatitic major element compositions and their varying radiogenic isotope signatures (Fig. 1a and Fig. 4; Table S-1 and S-3).

Previously published Sr-Nd ( $\pm$ Pb) isotope data are limited to 5 additional microinclusion-bearing diamonds from Canada, Botswana and Congo, all with silicic to low-Mg carbonatitic HDF compositions (Klein-BenDavid *et al.*, 2010, 2014; Timmerman *et al.*, 2019). Figure 4 shows that these HDFs overlap and expand the isotopic trends of the studied HDFs towards more unradiogenic Nd and radiogenic Sr and Pb compositions. These Sr-Nd isotope ratios overlap sediments derived from old continental crust (Goldstein and Jacobsen, 1987), suggesting their possible contribution to the formation of HDFs through subduction. Such a connection is consistent with the correlation between La/Nb and isotopes (Fig. 2c and Fig. 6e in Klein-BenDavid *et al.*,

2014), implying the involvement of a recycled component, and may also explain the radiogenic  $^{207}\text{Pb}/^{204}\text{Pb}$  signature of all of these HDFs (Fig. 4c, Fig. S-1 and Fig. 8 of Klein-BenDavid *et al.*, 2014). Remarkably, the  $^{207}\text{Pb}/^{204}\text{Pb}$  vs.  $^{206}\text{Pb}/^{204}\text{Pb}$  composition of the HDFs define a positive trend (Fig. 4c). Klein-BenDavid *et al.* (2014) suggested that the Pb isotope signature of the most radiogenic HDF indicates a multi-stage evolution of its source, characterised by an Archean enrichment event, which increased the U/Pb ratios ( $\mu$ ), followed by a more recent event that led to lower  $\mu$ . Although there is no unique solution to explain the data, such a scenario fits all of the HDF data. Thus, the  $^{207}\text{Pb}/^{204}\text{Pb}$  vs.  $^{206}\text{Pb}/^{204}\text{Pb}$  trend may be interpreted as an age that corresponds to  $3214 \pm 369$  Ma (Fig. 4c). However, this trend is more likely the manifestation of mixing of two isotopic endmember source components that differ in age significantly. Calculated Nd  $T_{\text{DM}}$  model ages for the HDFs sources suggest an age range between 0.5 and 1.8 Ga (although these ages are minimum estimates because HDF formation produces LREE enrichment which reduces the model ages; Goldstein *et al.*, 1984). The most unradiogenic HDF sample reported by Klein-BenDavid *et al.* (2014) yields a  $T_{\text{DM}}$  of 2.6 Ga.

In summary, the relationships between isotope and trace element ratios of silicic to low Mg-carbonatitic HDFs indicate the involvement of two distinct eclogite/pyroxenite-dominated sources within the continental lithosphere: one with a relatively primitive Sr-Nd isotope composition and another with unradiogenic Nd and radiogenic Sr and Pb isotope ratios. We propose that the latter source reflects an old metasomatic event in the Canadian continental root by fluid addition from a subducting slab (most probably involving the Slave Craton in the Paleoproterozoic,  $\geq 1.8$  Ga, e.g., Wopmay collisional event). Near-solidus melting of this source during a subsequent tectono-magmatic event led to the formation of HDFs with unradiogenic Nd and radiogenic Sr and Pb isotope ratios. Simultaneous melting of a more primitive source introduced HDFs with less enriched Sr-Nd isotope signature, and mixing of the two HDF endmember components formed silicic to low-Mg carbonatitic HDFs with the observed range of Sr-Nd-Pb isotope compositions (Fig. 4). Formation of either HDF endmember in one of the sources, which percolates through and interacts with the other source, would lead to equivalent results. Either way, the HDFs' host diamonds crystallised during this event. The relatively short mantle residence time of these diamonds, indicated by their unaggregated nitrogen, suggests that the Sr-Nd-Pb isotopic signature of the subducting component, most notably the relatively elevated  $^{207}\text{Pb}/^{204}\text{Pb}$  was formed in, or was added to, the cratonic continental lithosphere long before HDF formation and inclusion in diamonds. Comparable isotope-trace element relationships in silicic- to low-Mg carbonatitic-bearing diamonds from different continents suggest that the same processes, including sediment subduction, impacted other SCLM provinces producing the source of diamond-forming fluids.

## Acknowledgements

We thank S. Jockusch for help with the ablations of diamond-in-water, O. Elazar for help with column chemistry and Sr isotope analyses, and M. Schrauder for the donation of diamonds used in this study. We thank Graham Pearson, Emma Tomlinson and an anonymous reviewer, as well as GPL Editor Ambre Luguët for detailed and constructive reviews. Y.W. acknowledges support by ISF Grants No. 2015/18 and 779/22, NSF Grant EAR-1348045 and Europlanet 2020 RI Grant 18-EPN5-002. Europlanet 2020 RI has received funding from the European

Union's Horizon 2020 research and innovation programme under grant agreement No. 654208.

Editor: Ambre Luguët

## Additional Information

Supplementary Information accompanies this letter at <https://www.geochemicalperspectivesletters.org/article2329>.



© 2023 The Authors. This work is distributed under the Creative Commons Attribution Non-Commercial No-Derivatives 4.0

License, which permits unrestricted distribution provided the original author and source are credited. The material may not be adapted (remixed, transformed or built upon) or used for commercial purposes without written permission from the author. Additional information is available at <https://www.geochemicalperspectivesletters.org/copyright-and-permissions>.

**Cite this letter as:** Weiss, Y., Koornneef, J.M., Davies, G.R. (2023) Sr-Nd-Pb isotopes of fluids in diamond record two-stage modification of the continental lithosphere. *Geochem. Persp. Lett.* 27, 20–25. <https://doi.org/10.7185/geochemlet.2329>

## References

- AKAGI, T., MASUDA, A. (1988) Isotopic and elemental evidence for a relationship between kimberlite and Zaire cubic diamonds. *Nature* 336, 665–667. <https://doi.org/10.1038/336665a0>
- AULBACH, S., HEAMAN, L.M., JACOB, D.E., VIJJOEN, K.S. (2019) Ages and sources of mantle eclogites: ID-TIMS and in situ MC-ICPMS Pb-Sr isotope systematics of clinopyroxene. *Chemical Geology* 503, 15–28. <https://doi.org/10.1016/j.chemgeo.2018.10.007>
- BECKER, M., LE ROEX, A.P. (2006) Geochemistry of South African on- and off-craton, Group I and Group II kimberlites: Petrogenesis and source region evolution. *Journal of Petrology* 47, 673–703. <https://doi.org/10.1093/petrology/egj089>
- COHEN, R.S., O'NIONS, R.K., DAWSON, J.B. (1984) Isotope geochemistry of xenoliths from East Africa: Implications for development of mantle reservoirs and their interaction. *Earth and Planetary Science Letters* 68, 209–220. [https://doi.org/10.1016/0012-821X\(84\)90153-5](https://doi.org/10.1016/0012-821X(84)90153-5)
- DAVIES, G., LLOYD, F. (1986) Sub-continental lithosphere beneath Katew-Kikorongo, SW Uganda. *International Kimberlite Conference: Extended Abstracts* 4, no. 1, 229–231. <https://doi.org/10.29173/ikc1126>
- DAWSON, J.B. (1984) Contrasting Types of Upper-Mantle Metasomatism? In: KORNPROBST, J. (Ed.), *Developments in Petrology*, 11, 289–294. <https://doi.org/10.1016/B978-0-444-42274-3.50030-5>
- FRASER, K.J., HAWKESWORTH, C.J., ERLANK, A.J., MITCHELL, R.H., SCOTT-SMITH, B.H. (1985) Sr, Nd and Pb isotope and minor element geochemistry of lamp-roites and kimberlites. *Earth and Planetary Science Letters* 76, 57–70. [https://doi.org/10.1016/0012-821X\(85\)90148-7](https://doi.org/10.1016/0012-821X(85)90148-7)
- GOLDSTEIN, S.J., JACOBSEN, S.B. (1987) The Nd and Sr isotopic systematics of river-water dissolved material: Implications for the sources of Nd and Sr in seawater. *Chemical Geology: Isotope Geoscience Section* 66, 245–272. [https://doi.org/10.1016/0168-9622\(87\)90045-5](https://doi.org/10.1016/0168-9622(87)90045-5)
- GOLDSTEIN, S.L., O'NIONS, R.K., HAMILTON, P.J. (1984) A Sm-Nd isotopic study of atmospheric dusts and particulates from major river systems. *Earth and Planetary Science Letters* 70, 221–236. [https://doi.org/10.1016/0012-821X\(84\)90007-4](https://doi.org/10.1016/0012-821X(84)90007-4)
- HART, S.R., HAURI, E.H., OSCHMANN, L.A., WHITEHEAD, J.A. (1992) Mantle plumes and entrainment – isotopic evidence. *Science* 256, 517–520. <https://doi.org/10.1126/science.256.5056.517>
- JACOB, D. (2004) Nature and origin of eclogite xenoliths from kimberlites. *Lithos* 77, 295–316. <https://doi.org/10.1016/j.lithos.2004.03.038>
- KEMPE, Y., WEISS, Y., CHINN, I., NAVON, O. (2021) Multiple metasomatic diamond-forming events in a cooling lithosphere beneath Voorspoed, South Africa. *Lithos*, 106285. <https://doi.org/10.1016/j.lithos.2021.106285>
- KLEIN-BENDAVID, O., PEARSON, D.G., NOWELL, G.M., OTTLEY, C., MCNEILL, J.C.R., CARTIGNY, P. (2010) Mixed fluid sources involved in diamond growth



- constrained by Sr–Nd–Pb–C–N isotopes and trace elements. *Earth and Planetary Science Letters* 289, 123–133. <https://doi.org/10.1016/j.epsl.2009.10.035>
- KLEIN-BENDAVID, O., PEARSON, D.G., NOWELL, G.M., OTTLEY, C., MCNEILL, J.C.R., LOGVINOVA, A., SOBOLEV, N.V. (2014) The sources and time-integrated evolution of diamond-forming fluids – Trace elements and isotopic evidence. *Geochimica et Cosmochimica Acta* 125, 146–169. <https://doi.org/10.1016/j.gca.2013.09.022>
- MCDONOUGH, W.F., SUN, S.S. (1995) The composition of the Earth. *Chemical Geology* 120, 223–253. [https://doi.org/10.1016/0009-2541\(94\)00140-4](https://doi.org/10.1016/0009-2541(94)00140-4)
- RUDNICK, R.L. (1990) Nd and Sr isotopic compositions of lower-crustal xenoliths from north Queensland, Australia: Implications for Nd model ages and crustal growth processes. *Chemical Geology* 83, 195–208. [https://doi.org/10.1016/0009-2541\(90\)90280-K](https://doi.org/10.1016/0009-2541(90)90280-K)
- SMITH, E.M., KOPYLOVA, M.G., NOWELL, G.M., PEARSON, D.G., RYDER, J. (2012) Archean mantle fluids preserved in fibrous diamonds from Wawa, Superior craton. *Geology* 40, 1071–1074. <https://doi.org/10.1130/G33231.1>
- STACHEL, T., HARRIS, J.W. (2008) The origin of cratonic diamonds — Constraints from mineral inclusions. *Ore Geology Reviews* 34, 5–32. <https://doi.org/10.1016/j.oregeorev.2007.05.002>
- STRACKE, A. (2012) Earth's heterogeneous mantle: A product of convection-driven interaction between crust and mantle. *Chemical Geology* 330, 274–299. <https://doi.org/10.1016/j.chemgeo.2012.08.007>
- TAYLOR, W.R., CANIL, D., MILLEDGE, H.J. (1996) Kinetics of Ib to IaA nitrogen aggregation in diamond. *Geochimica et Cosmochimica Acta* 60, 4725–4733. [https://doi.org/10.1016/S0016-7037\(96\)00302-X](https://doi.org/10.1016/S0016-7037(96)00302-X)
- THOMPSON, R.N., RICHES, A.J.V., ANTOSHECHKINA, P.M., PEARSON, D.G., NOWELL, G.M., OTTLEY, C.J., DICKIN, A.P., HARDS, V.L., NGUNO, A.-K., NIKU-PAAVOLA, V. (2007) Origin of CFB Magmatism: Multi-tiered Intracrustal Picrite–Rhyolite Magmatic Plumbing at Spitzkoppe, Western Namibia, during Early Cretaceous Etendeka Magmatism. *Journal of Petrology* 48, 1119–1154. <https://doi.org/10.1093/petrology/egm012>
- TIMMERMAN, S., YEOW, H., HONDA, M., HOWELL, D., JAQUES, A.L., KREBS, M.Y., WOODLAND, S., PEARSON, D.G., ÁVILA, J.N., IRELAND, T.R. (2019) U-Th/He systematics of fluid-rich ‘fibrous’ diamonds – Evidence for pre- and syn-kimberlite eruption ages. *Chemical Geology* 515, 22–36. <https://doi.org/10.1016/j.chemgeo.2019.04.001>
- TURNER, S., TURNER, M., BOURDON, B., COOPER, K., PORCELLI, D. (2021) Extremely young melt infiltration of the sub-continental lithospheric mantle. *Physics of the Earth and Planetary Interiors* 313, 106325. <https://doi.org/10.1016/j.pepi.2019.106325>
- WEISS, Y., GRIFFIN, W.L., NAVON, O. (2013) Diamond-forming fluids in fibrous diamonds: The trace-element perspective. *Earth and Planetary Science Letters* 376, 110–125. <https://doi.org/10.1016/j.epsl.2013.06.021>
- WEISS, Y., MCNEILL, J., PEARSON, D.G., NOWELL, G.M., OTTLEY, C.J. (2015) Highly saline fluids from a subducting slab as the source for fluid-rich diamonds. *Nature* 524, 339–342. <https://doi.org/10.1038/nature14857>
- WEISS, Y., GOLDSTEIN, S.L. (2018) The involvement of diamond-forming fluids in the metasomatic ‘cocktail’ of kimberlite sources. *Mineralogy and Petrology*, 1–19. <https://doi.org/10.1007/s00710-018-0613-8>
- WEISS, Y., CZAS, J., NAVON, O. (2022a) Fluid inclusions in fibrous diamonds. *Reviews in Mineralogy and Geochemistry* 88, 475–532. <https://doi.org/10.2138/rmg.2022.88.09>
- WEISS, Y., JOCKUSCH, S., KOORNNEEF, J.M., ELAZAR, O., DAVIES, G.R. (2022b) Laser ablation of ‘diamonds-in-water’ for trace element and isotopic composition analysis. *Journal of Analytical Atomic Spectrometry* 37, 1431–1441. <https://doi.org/10.1039/D2JA00088A>
- XU, W.-L., GAO, S., YANG, D.-B., PEI, F.-P., WANG, Q.-H. (2009) Geochemistry of eclogite xenoliths in Mesozoic adakitic rocks from Xuzhou-Suzhou area in central China and their tectonic implications. *Lithos* 107, 269–280. <https://doi.org/10.1016/j.lithos.2008.11.004>
- ZINDLER, A., HART, S. (1986) Chemical Geodynamics. *Annual Review of Earth and Planetary Sciences* 14, 493–571. <https://doi.org/10.1146/annurev.ea.14.050186.002425>

